Experimental and Theoretical Study on the Structure and Formation Mechanism of [C 6 H 5 Cu m] − (m = 1−3)

ARTICLE *in* THE JOURNAL OF PHYSICAL CHEMISTRY A · JUNE 2007

Impact Factor: 2.69 · DOI: 10.1021/jp066750y · Source: PubMed

6 AUTHORS, INCLUDING:

Xiang Zhang
Shanxi Teachers University
21 PUBLICATIONS **194** CITATIONS

SEE PROFILE

Experimental and Theoretical Study on the Structure and Formation Mechanism of $[C_6H_5Cu_m]^-$ ($m = 1-3$)

Xiao-Jing Liu,[†] Xiang Zhang,[†] Ke-Li Han,*[,†] Xiao-peng Xing,[‡] Shu-tao Sun,[‡] and Zi-Chao Tang*[,†,‡]

State Key Laboratory of Molecular Reaction Dynamics, Dalian Institute of Chemical Physics, Chinese Academy of Sciences, Dalian 11602, China, and State Key Laboratory of Molecular Reaction Dynamics, Center of Molecular Science, Institute of Chemistry, Chinese Academy of Sciences, Beijing 100080, China

Received: October 14, 2006; In Final Form: February 26, 2007

The important intermediate phenyl−copper metal complexes $[C_6H_5Cu_m]^-$ ($m = 1-3$), which are produced from the reactions between copper metal clusters formed by laser ablation and the benzene molecules seeded in argon carrier gas, are studied by photoelectron spectroscopy(PES) and density functional theory (DFT). Their structures and bonding patterns are investigated, which results in the conclusion that C_6H_5 groups bond perpendicularly on copper clusters through Cu−C σ bond. The formation mechanism of these complexes has been studied at B3LYP//6-311G(d, p)/Lanl2dz level. Direct insertion reaction between $[Cu_m]^-$ and C_6H_6 yields intermediate complex $[C_6H_5Cu_mH]^-$, and then eliminates the H atom, or releases the H atom to other neutral Cu atoms or anionic Cu ions via H abstraction reaction. The first step is the rate-limiting step with C−H activation and cleavage, and H abstraction by neutral Cu atom is the most energetically favorable pathway for the final step. Moreover, the complex $[C_6H_5Cu_2]^-$ is ascertained to be easier to be generated than $[C_6H_5Cu_3]^-$ and $[C_6H_5Cu]^-$, which are in excellent agreement with the experimental results.

1. Introduction

Studies on the chemical interactions between metal clusters and organic molecules could provide useful information for further understanding some important heterogeneous catalytic processes in the organometallic chemistry field.[1−4] Additionally, verifying the structures and properties of these formed complexes can develop a microscopic level description of many heterogeneous catalysis reactions (for example the Ullmann reaction[5]). Since the active points in the catalysis reactions or the Raman enhancement principles are localized near the edges or the defects of metal surfaces, study on the fragments adsorbed on small metal clusters can be a promising platform.

In recent years, a lot of experimental[6−12] and theoretical[13−16] investigations on the interaction of metal clusters with benzene have been carried out because the gas-phase reaction is suitable model system to shed light on the reaction mechanism.[17−19] All these results indicate that a phenyl group on orderly metal surfaces has the slightly titled configuration through metal−carbon bond. However, the species of phenyl group coupled on metal atoms or clusters are a kind of very important intermediates in catalytic processes.[20,21]

In this paper, we report the first observation and characterization of phenyl groups coupled on small copper metal clusters $[Cu_m]^-$ ($m = 1-3$) in gas phase using mass spectrometry and anion photoelectron spectroscopy. The bonding structures of these complexes are obtained by a combination of experimental and theoretical studies. Furthermore, the systematically theoretical investigation of formation mechanism of these complexes $[Cu_mC_6H_5]^-$ ($m = 1-3$) in the ground state is performed. The reaction mechanisms are shown in Scheme 1, in which the third pathway is turned out to be the most energetically favorable one. All these results give a clear diagram about their structures, the bond interactions and the formation processes.

SCHEME 1: Possible Formation Mechanisms of $[C_6H_5-Cu_m]^-$ ($m = 1-3$) Complexes We Suggested

$$C_6H_6+[Cu_m]^- \longrightarrow [C_6H_5\text{-}Cu_mH]^- \longrightarrow [C_6H_5\text{-}Cu_m]^- + H \quad (1)$$

$$\xrightarrow{[Cu]^-} [C_6H_5\text{-}Cu_m]^- + [CuH]^- \quad (2)$$

$$\xrightarrow{Cu} [C_6H_5\text{-}Cu_m]^- + CuH \quad (3)$$

2. Experimental Methods

Details of the apparatus have been published elsewhere.[22] Here a brief description is presented. The pure copper metal disk targets are ablated by a pulsed laser beam (532 nm Nd: YAG laser, 10 mJ/pulse), and the targets are rotated during the experiment. The laser-induced plasma is mixed with benzene (analytical reagent) in a channel, and the benzene is seeded in argon (purity 99.99%) carrier gas delivered by a pulsed valve with a backing pressure of about 400 kPa. The volume ratio of benzene in the mixed gas is about 0.2%. The phenyl−copper metal clusters formed are entrained with the carrier gas and undergo a supersonic expansion. After passing a skimmer, all products are into the accelerating area, and then negatively charged clusters are extracted perpendicularly from the collimated cluster beam for size analysis by a reflectron time-of-flight mass spectrometer. The resolution ($M/\Delta M$) of the mass spectrometer is about 2000, so it is easy to resolve the number of the hydrogen atoms in the products. The products of interest are mass selected and photodetached by a XeCl excimer laser (308 nm), respectively. Photoelectrons are measured by a magnetic-bottle time-of-flight analyzer and calibrated by the

* To whom correspondence should be addressed.
† Dalian Institute of Chemical Physics.
‡ Institute of Chemistry.

10.1021/jp066750y CCC: $37.00
Published on Web 04/10/2007

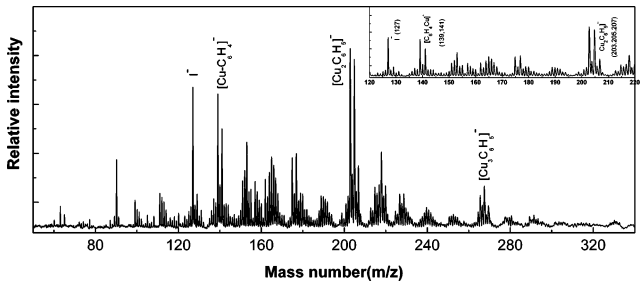

Figure 1. Typical mass spectra of the anion products by laser vaporization/ionization of copper metal samples into a mixture of argon and benzene. The inserts in A and B shows the enlarged part of the spectra, which contain $[Cu_m-C_6H_5]^-$ products and iodine anion mass peak.

known spectra of Ag^- and Au^-. The energy resolution of the instrument is approximately 70meV for 1 eV electrons.

3. Computational Methods

All the calculations are accomplished with the set of Gaussian03 program.[23] All full optimizations of geometries and harmonic vibration frequency calculations of the reactants, transition states, intermediates and products are performed with the method of three-parameter hybrid functional of Becke using the Lee−Yang−Parr correlation functional (B3LYP)[24] of hybrid density functional theory (DFT). The standard basis set 6-311G-(d, p) is used for C and H atoms, while the Lanl2dz ECP[25] basis set is adopted for Cu atom. It has been shown that these theoretical methods are currently the most accurate and appropriate approach for studying the structure and energetics of organocopper molecules and the copper clusters.[26−28] All transition states are located without imposing any constraints during the geometry optimization process and are confirmed by one imaginary mode from vibrational analysis calculations. In all cases the vibrational mode with the imaginary frequency is verified to connect a specific pair of stationary points (reactants, products, or minima associated to intermediate species) by performing the necessary intrinsic reaction coordinate (IRC) calculations with step size of 5 (in units of 0.01 $amu^{1/2}$ bohr). All energies reported here are corrected with the zero-point vibrational energy (ZPVE). Since recent reports[29,30] seem to indicate that the charges evaluated using the atomic polar tensors (APT) are more representative of the electron density distributions and are also relatively insensitive to basis set variations, to carry out charge analysis, we have computed the APT charges from the calculated wave functions of the optimized geometries of these complexes.

4. Results and Discussion

4.1. Mass Spectra. As shown in Figure 1, anion phenyl−copper complexes $[Cu_mC_6H_5]^-$ are the dominant products of the reactions. The I^- peaks presented (coming from the trace CH_3I mixed in argon purposively) are very helpful for assignment of the products. An exception is that the produced $[Cu-C_6H_4]^-$ is more than $[Cu-C_6H_5]^-$. This can be an evidence that copper atom tends to show bivalent rather than univalent in its organic compounds.

4.2. Photoelectron Spectra. The photoelectron spectra represent transitions from the ground of the anions to the ground and excited electronic states of the neutrals. The anions are in their electronic ground state because they are cooled in a supersonic expansion. When the photodetachment process happens, this process is much faster compared with the movements of the nuclei. Consequently, PES provides the

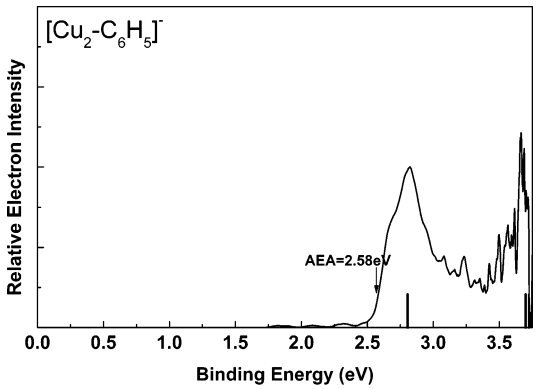

Figure 2. Photoelectron spectra of $[Cu_2-C_6H_5]^-$ at 4.03 eV photon energy. (The arrows indicate the intensity 20% of that of the lowest maximum in each spectrum and these were approximately considered to be the adiabatic EAs. The stick spectra are the occupied energy levels from the DFT calculations in the spin−orbit option by aligning the highest occupied level(s) with the threshold feature.

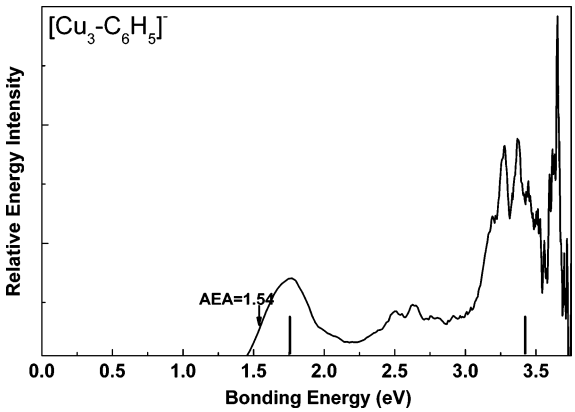

Figure 3. The same as in Figure 2, except for $[Cu_3-C_6H_5]^-$.

TABLE 1: EAs (eV) of $[Cu_m-C_6H_5]$ ($m = 1-3$) and Their Corresponding Pure Metal Species

	Cu_m	$(Cu_m-C_6H_5)$	
copper metal species	EA[a]	EA (exp)[b]	EA cal)
Cu_1	1.23		0.60
Cu_2	0.84	2.58	2.37
Cu_3	2.27	1.54	1.53

[a] Derived from PES experiments in refs 31 and 32. [b] The error bars were within 0.10 eV.

electronic and vibrational (if the resolution is enough) information of the neutral species corresponding to the anionic cluster geometry. EA is defined as the energy of the origin transition between the ground state of the anion and the ground state of the neutral.

Figures 2 and 3 show the PES results of $[Cu_m-C_6H_5]^-$ ($m = 2, 3$) at 308 nm photon ($h\nu \approx 4.03$ eV). Their electron affinities (EAs) of $C_6H_5Cu_m$ ($m = 1-3$) and the corresponding pure copper metal species[31,32] are presented in Table 1. The EAs value of calculated by DFT method is in excellent agreement with that determined in the experiments. It can be seen that the C_6H_5-Cu_3 exhibits lower electron binding energy and large energy gap, which indicate that the neutral cluster is closed-shell, and its highest-occupied-molecular orbital (HOMO) is occupied by two electrons, so the charging electron, which makes the species negative, would occupy the lowest-unoccupied molecular orbital (LUMO). However, the $C_6H_5Cu_2$ shows higher electron binding energy, which suggests that it is open-shell electronic systems.

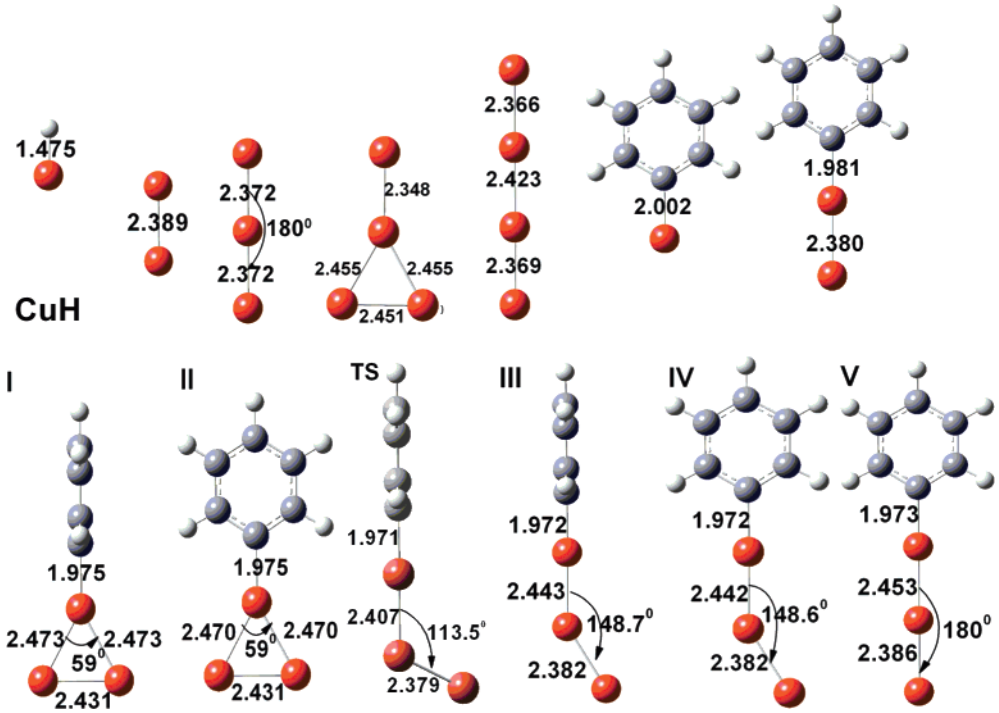

Figure 4. Optimized structures with some important bond lengths for the complexes of $[Cu_m]^-$, $[C_6H_5Cu_m]^-$ ($m = 1-3$) CuH.

TABLE 2: Point Group and Energetic Characteristics for the Five Kind Isomers of $[C_6H_5Cu_3]^-$ and Transition State of Geometry Conversion between Them

$[C_6H_5Cu_3]^-$ isomers	I	II	TS	III	IV	V
point group	C_{2v}	C_{2v}	C_1	C_s	C_1	C_{2v}
E_0 (Hartree)	−820.146045	−820.145962	−820.137614	−820.138258	−820.138216	−820.138174
relative energy ΔE	0	0.0521	5.291	4.886	4.913	4.939

Its HOMO is occupied by only one electron, so the charging electron would occupy the other position of the HOMO, which makes their EAs higher. This can be explained by the electron pairing effect, just like the pure copper clusters, in which the EA of the odd-numbered pure copper cluster is larger than that of an even one.[33−36] Because each metal atom in the clusters contributes a single s valence electron to the bonding orbitals, the odd-numbered pure coinage metal anionic clusters are closed-shell. The electron in a doubly occupied HOMO will feel a stronger effective core potential due to less effect of the electron screening for electrons in the same orbital than for the inner shell electrons. By this analysis, the C_6H_5 group acts like an additional copper atom in these complexes that it contributes a single electron to bond with the metal fragment and the most possible bond is C−Cu σ.

4.3. Structures of Stable Species. To support the experimental result, the structures of $[Cu_m]^-$ ($m = 2-4$) and $[C_6H_5Cu_m]^-$ ($m = 1-3$) are optimized by DFT method. The optimized stable ground-state structures of these complexes are presented in Figure 4. The ground-state $[Cu_3]^-$ is optimized to be only linear-structure without triangle-structure, in accordance with the earlier studies.[33−36] The ground-state $[Cu_4]^-$ is optimized to be two isomers: a Y-shape structure and a linear form. The Y-shape structure is 2.0 kcal/mol lower in energy than the linear form. All the Cu−Cu bond lengths of $[Cu_m]^-$ obtained here are consistent with the reported data by experiment.[33−36] The optimized structures of $[C_6H_5Cu]^-$ and $[C_6H_5Cu_2]^-$ belong to C_{2v} symmetry, in which the C_6H_5 group couples with the Cu atom through C−Cu bond and C−Cu−Cu are in a line with the same plane of the C_6H_5 group. The complex $[C_6H_5Cu_3]^-$ has five different isomers (I−V), and the corresponding structures and energy characteristics are summarized in Table 2. The one of lowest-energy is a Y-shaped structure with C_{2v} symmetry, where the C_6H_5 group is perpendicular to the plane of Cu_3 cluster. The energetically closest isomer is also a Y-shape with C_{2v} symmetry, where the C_6H_5 group rotates to the same plane of Cu_3 cluster. The energy difference between these two Y-shaped structures is only 0.05 kcal/mol. All of other three structures are almost 4.9 kcal/mol higher in energy than the lowest-energy structure. And the activation energy barriers from the structures (I, II) to structures (III, IV, V) are about 5.2 kcal/mol. The geometry of this transition state (TS) is also displayed in Figure 4. Therefore, the structures (III, IV, V) can be safely ruled out only for reasons in energy. Very recently,[20] it has been ascertained that the structures of $[C_6H_5Ag_3]^-$ and $[C_6H_5Au_3]^-$ are similar to the above two geometries by the experiment of photoelectron spectroscopy and relativistic DFT calculation.

Moreover, the assignment of the most possible structures is given on the base of relative energies and the comparisons between the theoretically calculated DOS and the experimental PES spectra. The structural assignment method has been widely used in cluster studies.[37−43] The theoretical density of state (DOS) is shifted by setting the HOMO level of the spectra to give the negative of the DOS value for the complex. This is called the theoretically generalized Koopman theorem (GKT)[44]-shifted DOS.[40] The comparisons of theoretical results with experimental PES of $[Cu_m-C_6H_5]^-$ ($m = 2, 3$) are shown in Figures 2−3. Here it should be noticed that in comparison of the DOS spectra with the PES spectra, the importance is the electron binding energy corresponding to the each feature and not the relative intensity. The relative intensity also depends on other factors such as the unknown orbital-dependent photodetachment cross section. So here the DOS is plotted as the stick spectrum by aligning the HOMO level of anions with the

threshold peak, instead of the fitted DOS spectra. It can be seen that the energy gap between the HOMO levels in the DOS spectrum agrees reasonably well with the experimental PES spectrum. Furthermore, the structures I and II of $[C_6H_5Cu_3]^-$ are provided by the HOMO−LUMO difference of structures I (1.33 eV) and II (1.36 eV), which best match the gap in PES.

From the structure investigations above, the geometries of $[C_6H_5Cu_{m-1}]^-$ ($m = 2-4$) correspond to those of $[Cu_m]^-$ ($m = 2-4$), respectively, in which the C_6H_5 group acts just like an additional copper atom in the clusters and contributes a single electron to bond with the copper fragment. The C−Cu bond lengths obtained here are similar to each other and also similar to the results of another theoretical study.[45] The small energy difference between the two isomers of $[C_6H_5Cu_3]^-$ indicates that the C_6H_5 group could rotate freely through C−Cu bond. All of these results manifest that the C_6H_5 group binds on the copper metal clusters though C−Cu σ bond.

4.4. Formation Mechanism of $[C_6H_5Cu_m]^-$ ($m = 1-3$). As shown in Scheme 1, one can see that the formation process of $[C_6H_5Cu_m]^-$ ($m = 1-3$) is a two-step reaction. The first step is an insertion of $[Cu_m]^-$ into the C−H bond of C_6H_6 to yield intermediate complex $[C_6H_5Cu_mH]^-$. The followed step is the generation of $[C_6H_5Cu_m]^-$ with the release of H, in which three possible pathways are involved. Figure 5 presents the optimized structures with some key bond lengths of various reaction species along the reaction pathway of $[C_6H_5Cu_m]^-$ ($m = 1-3$) formation.

4.4.1. Generation of Intermediate $[C_6H_5Cu_mH]^-$ ($m = 1-3$). As shown in Figure 6 about the formation mechanism of $[C_6H_5CuH]^-$ (IM1b), at the initial stage of reaction, Cu^- anion moves to benzene molecule forming a reactant complex with a bonding energy of 7.29 kcal/mol. And then Cu^- is inserted into C−H bond, which results in the formation of intermediate $[C_6H_5CuH]^-$ (IM1b). This process proceeds via a transition state (TS1a) with energy barrier of 49.2 kcal/mol, which is confirmed by the IRC calculation.

Figure 7 presents the reaction of $[Cu_2]^-$ with benzene, at first, the planar C_{2v} symmetry complex (IM2a) and C_s symmetry complex (IM2b) can be formed. IM2a is more stable than the reactants by 4.51 kcal/mol, where two Cu atoms interact with two H atoms of benzene, respectively; the energy of IM2b is 1.15 kcal/mol higher than that of the reactants, and then one Cu atom interacts with C1−H7 bond of benzene to form IM2c through a transition state (TS2b) with an energy barrier of 26.4 kcal/mol. IM2c is the most stable species in this reaction channel, in which H7 acts as a bridge between the two Cu atoms. However, by scanning the Cu13−H7 distance, a linear configuration species IM2d could be afforded, which is 7.71 kcal/mol higher in energy than IM2c. In this process, H migration is accompanied by a displacement of Cu14, via a transition state (TS2c) of 14.3 kcal/mol barrier.

The formation mechanism of $[C_6H_5Cu_3H]^-$ (IM3b) is shown in Figure 8. Three Cu atoms in $[Cu_3]^-$ are not equivalent each other, where negative charge mostly is distributed on the terminal Cu atoms and the central Cu atom is of positive charge. In view of the unequivalence of the central Cu atom and the terminal Cu atoms in $[Cu_3]^-$, two competitive reaction pathways of $[Cu_3]^-$ interacting with the benzene are considered. One is the central atom Cu13 attacking the C1 atom of benzene. Initially, a C_s symmetry complex (IM3a) is formed, which is more stable than the reactants by 3.21 kcal/mol. Then the central atom Cu13 interacts with the C1−H7 bond of benzene, which results in the cleavage of the C1−H7 bond and formation of IM3b, via TS3a of 31.9 kcal/mol barrier. In this process, H7 transfers to Cu14 directly. The other pathway is the terminal atom Cu14 in $[Cu_3]^-$ attacking the C1 of benzene to give rise to another C_s symmetry complex (IM3a′), which is 1.94 kcal/mol more stable than the reactants. And an insertion of Cu14 into the C1−H7 bond yields the intermediate IM3b′, through a transition state (TS3a′) of 49.3 kcal/mol barrier. IM3b′ is the most stable species in this reaction pathway, in which H7 acts as a bridge between the Cu14 and Cu13 atoms. However, a migration of H7 from Cu14 to Cu13 evolves to yield species IM3b, through a transition state TS3b′ of 12.6 kcal/mol barrier, which is found by scanning the Cu14−H7 distance.

It can be observed that the generation of intermediate $[C_6H_5Cu_mH]^-$ ($m = 1-3$) is a key step with the C1−H7 bond activation because of its large bond dissociation energy (109.1 kcal/mol). Then this reaction should take place easily. As listed in Tables 3−5, along the pathway of forming $[C_6H_5Cu_mH]^-$ ($m = 1-3$), the negative charge of $[Cu_m]^-$ ($m = 1-3$) is decreasing with increasing of the negative charges of benzene group and H7. Clearly, the delocalization of the negative charges from $[Cu_m]^-$ to the benzene molecule leads to the activation and cleavage of C1−H7 bond. Then an insertion of Cu into C1−H7 bond results in the formation C1−Cu and Cu−H7 bonds. However the modes of Cu^-, $[Cu_2]^-$ and $[Cu_3]^-$ attacking benzene are different from each other. For Cu^-, in view of the existing lone-pair electrons ($4s^2$) of Cu^-, it affords lone-pair electrons attacking H to form coordinate bond Cu−H. Once the Cu−H bond is formed, the C−H bond of benzene is activated through the electron transfer from Cu^- to the benzene. As to $[Cu_2]^-$, it has a single electron (σ^*) on the HOMO. Because the LUMO of benzene has a large orbital coefficient on the C atom (π^*), it is reasonable for $[Cu_2]^-$ to attack the C atom of benzene rather than H atom. In the intermediate $[C_6H_5CuHCu]^-$ (IM2c), the charge distribution of Cu13, H7 and Cu14 is 0.151, −0.272, −0.352, respectively, as presented in Table 3. It is obvious that the interaction between Cu13 and Cu14 is strengthening, which compels H7 to migrate from Cu13 to Cu14. As to $[Cu_3]^-$, it is necessary to mention that the distribution of negative charge is 0.124(Cu13), −0.562(Cu14), −0.562(Cu15), respectively. The central atom and the terminal atoms are not equivalent, which results in two possible attacking modes. Additionally, it could be seen that the charge of C1 of benzene is −0.028. It is reasonable that the central Cu13 (with positive charge of 0.124), as an electrophilic reagent, is easier to attack the C1 in benzene than Cu14 or Cu15 (with negative charge of −0.562). Therefore, this leads to the energy barrier of TS3a in the second channel lower than the corresponding one of TS3a′ in the first channel. On the other hand, it is worth to mention that, for all the reactions, to overcome the higher barrier of TSma ($m = 1-3$), excessive energy within hot metal clusters by laser vaporization is necessary.

The formation process of intermediate $[C_6H_5Cu_mH]^-$ is followed by the reaction of elimination of H atom. From the Figures 6−8, if the intermediate complexes $[C_6H_5Cu_mH]^-$($m = 1-3$) release H atom directly to yield the complexes $[C_6H_5Cu_m]^-$, the necessary energies are 78.7, 38.9, 64.8 kcal/mol, respectively. Additionally, $[C_6H_5Cu_2H]^-$ also could release CuH to generate $[C_6H_5Cu]^-$ with heat absorption of 38.8 kcal/mol, which is almost as much as the process of releasing H. It is worth mentioning that, although the excessive energy from Cu clusters generated by laser may be kept to this stage, it would be consumed by the reaction collisional deactivation with carrier gas. So this pathway is not easy to take place without enough

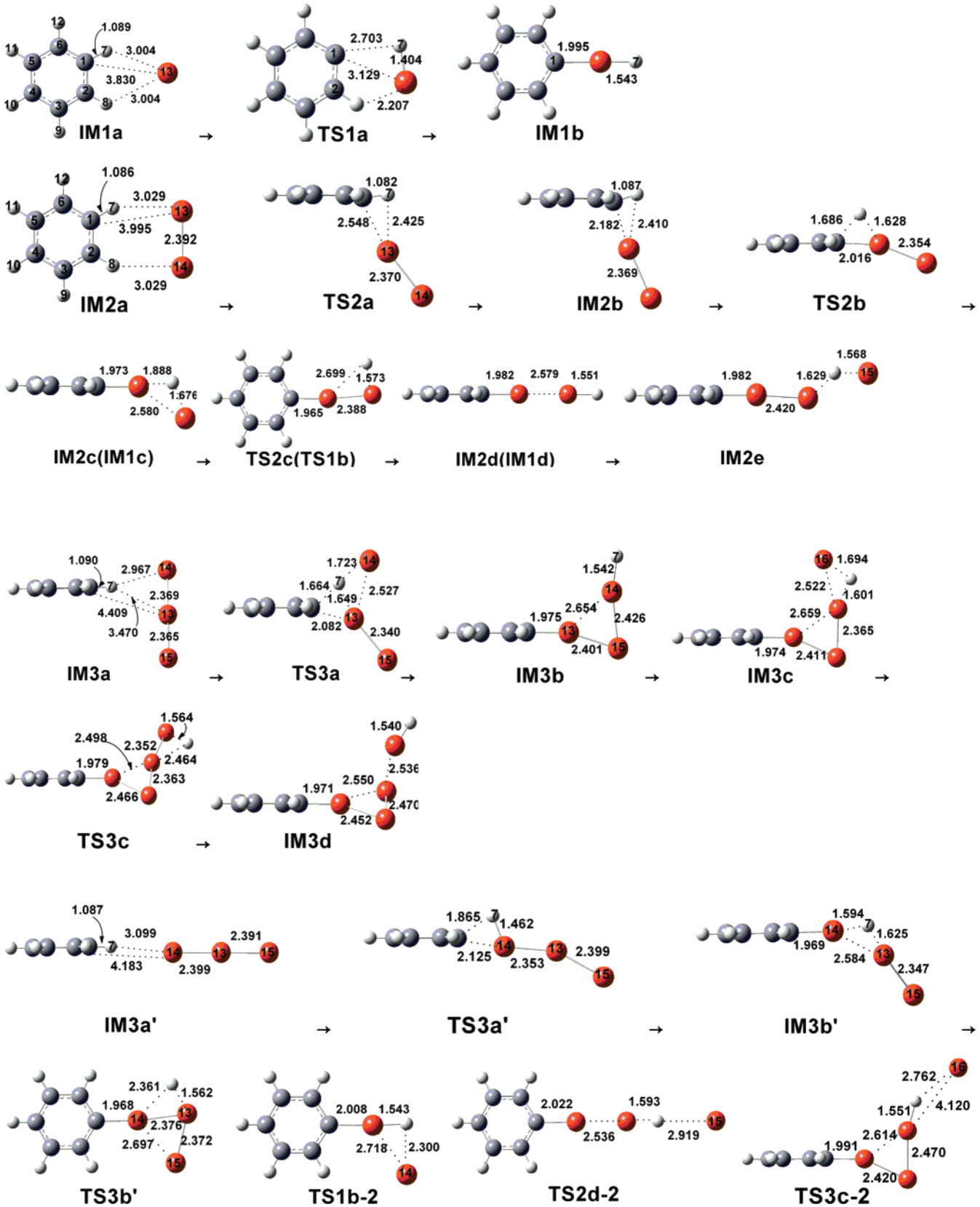

Figure 5. Optimized structures with some key bond lengths of various reaction species along the reaction pathway of $[C_6H_5Cu_m]^-$ ($m = 1-3$) formation.

energy. Maybe $[C_6H_5Cu_mH]^-$ could release the H through other ways. Considering there are a lot of laser-induced plasma of Cu, a few of H particles and other fragments in the system, it is suggested that the H7 of intermediate $[C_6H_5Cu_mH]^-$ could be eliminated by these species through a second-order reaction. However, the possibility of H7 removed by H particles and other fragments is considered to be very small, for these species are very few in the system, even the reaction is thermodynamic controlled. Therefore, the H7 removed by Cu plasmas is the most possible pathway.

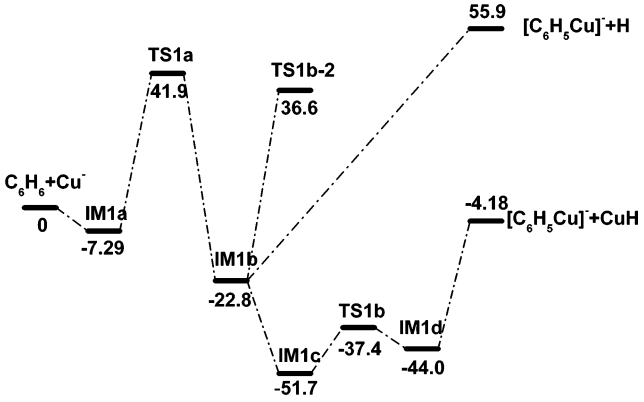

Figure 6. Relative energy profile along the reaction pathway of $[C_6H_5Cu]^-$ formation.

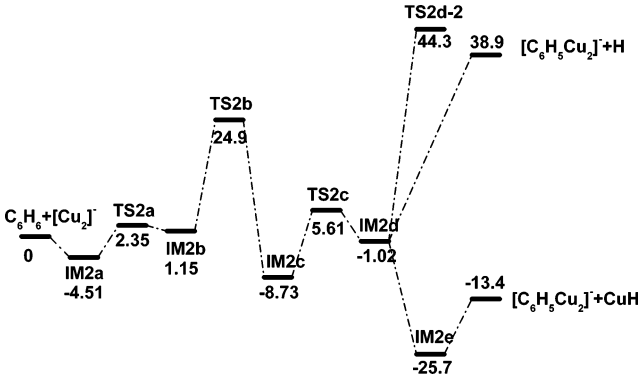

Figure 7. Relative energy profile along the reaction pathway of $[C_6H_5Cu_2]^-$ formation.

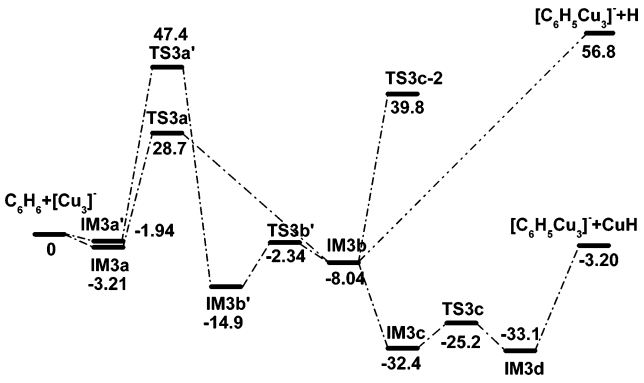

Figure 8. Relative energy profile along the reaction pathway of $[C_6H_5Cu_3]^-$ formation.

4.4.2. Removing of H by Cu or Cu⁻. As can be seen in Figures 6−8, the H7 atom is relatively easy to be eliminated by neutral Cu. Initially, when the neutral Cu nears to the intermediates $[C_6H_5Cu_mH]^-$ ($m = 1-3$), they form the complexes (IM1c, IM2e, IM3c), in which the H7 acts as a bridge between Cu atoms. All of these processes are exothermic with −28.9, −24.7, and −24.4 kcal/mol, respectively, which means the interactions between neutral Cu and $[C_6H_5Cu_mH]^-$ ($m = 1-3$) are very strong. After the formation of complexes $[C_6H_5Cu_mH-Cu]^-$, the H atom of $[C_6H_5Cu_mH]^-$ is abstracted by Cu to yield the product $[C_6H_5Cu_m]^-$ ($m = 1-3$) and CuH. In the reaction of $[C_6H_5CuH]^-$ and neutral Cu, the process of IM1c−TS1b−IM1d occurred, as well as the process of IM2c−TS2b−IM2d in the course of forming $[C_6H_5Cu_2H]^-$ IM2d (Figure 7). As far as the IM2e is concerned, it directly releases the CuH and $[C_6H_5Cu_2]^-$. The overall process is thermodynamically preferred for $\Delta E = -12.4$ kcal/mol. By scanning the Cu14−H7 distance, we found that IM3c could first form species IM3d, before releasing CuH and yielding the product. In this process, the migration of H is accompanied by a displacement of Cu16, through a transition state (TS3c) of 7.2 kcal/mol barrier. And then IM3d evolves to yield the product.

TABLE 3: Calculated APT Charge for All Stationary Points in the Course of $[C_6H_5Cu]^-$ Formation

	C_6H_5	C1	H7	Cu13	Cu14
Re	−0.028	−0.028	0.028	−1.000	
IM1a	−0.231	−0.140	0.146	−0.915	
TS1a	−0.732	−0.207	−0.084	−0.084	
IM1b	−0.586	−0.213	−0.500	0.087	
IM1c	−0.538	−0.112	−0.272	0.151	−0.352
TS1b	−0.622	−0.084	−0.208	0.315	−0.485
IM1d	−0.515	0.007	−0.423	0.004	−0.006
P	−0.406	0.033	−0.370	−0.584	0.370

TABLE 4: Calculated APT Charge for All Stationary Points in the Course of $[C_6H_5Cu_2]^-$ Formation

	C_6H_5	C1	H7	Cu13	Cu14	Cu15
Re	−0.028	−0.028	0.028	−0.500	−0.500	
IM2a	−0.113	−0.050	0.065	−0.474	−0.477	
TS2a	0.094	1.277	−0.121	−0.359	−0.612	
IM2b	−0.025	1.108	−0.162	−0.193	−0.617	
TS2b	−0.15	0.389	−0.357	0.001	−0.442	
IM2c	−0.538	−0.112	−0.272	0.151	−0.352	
TS2c	−0.622	−0.084	−0.208	0.315	−0.485	
IM2d	−0.515	0.007	−0.423	0.004	−0.006	
IM2e	−0.652	0.051	0.162	0.231	−0.340	−0.371
P	−0.593	−0.061	−0.370	0.136	−0.544	0.370

TABLE 5: Calculated APT Charge for All Stationary Points in the Course of $[C_6H_5Cu_3]^-$ Formation

	C_6H_5	C1	H7	Cu13	Cu14	Cu15	Cu16
Re	−0.028	−0.028	0.028	0.124	−0.562	−0.562	
IM3a	−0.102	−0.026	0.084	0.103	−0.540	−0.535	
TS3a	−0.679	−0.224	0.315	0.170	−0.394	−0.410	
IM3b	−0.553	−0.042	−0.441	0.165	0.087	−0.258	
IM3c	−0.556	−0.081	−0.176	0.209	0.085	−0.113	−0.450
TS3b	−0.586	−0.084	−0.069	0.306	0.028	−0.337	−0.342
IM3d	−0.538	−0.029	−0.487	0.245	−0.101	−0.245	0.125
P	−0.575	−0.048	−0.370	0.311	−0.367	−0.368	0.370
	−0.591	−0.068	−0.370	0.318	−0.363	−0.363	0.370

As listed in Tables 3−5, for the intermediates $[C_6H_5Cu_mH]^-$ ($m = 1-3$), the negative charge distributes predominantly in the benzene group and H7 atom. Although the neutral Cu atom is not a charged particle, and the outmost orbital is only filled with a single electron (4s). Because the HOMO of $[C_6H_5Cu_mH]^-$ has a large orbital coefficient on the H7 atom, it is reasonable for neutral Cu, as an electrophilic reagent, to attack the atom H7 rather than benzene group. The delocalization of the negative charge from $[C_6H_5Cu_mH]^-$ to the electrophilic reagent Cu gives rise to the stable complexes $[C_6H_5Cu_mH-Cu]^-$ ($m = 1-3$). In the course of forming complex $[C_6H_5Cu_2H-Cu]^-$, the charge of H7 is delocalized to Cu14 and Cu15 simultaneously, which results in the atoms Cu14 (−0.340) and Cu15 (−0.371) with the negative charge repelling with each other. Then the H7 is abstracted directly by the Cu15, which leads to the formation of CuH. Whereas, in the course of forming complexes of $[C_6H_5CuH-Cu]^-$ and $[C_6H_5Cu_3H-Cu]^-$, the charge of H7 is mostly delocalized to the neutral Cu, which strengthens the interactions between neutral Cu and the Cu near H. This results

in the migration of H to neutral Cu via a transition state before releasing CuH.

However, as shown in Figures 6−8, removing H7 of $[C_6H_5Cu_mH]^-$ ($m = 1-3$) by the anion Cu^-, initially, need to overcome the energy barrier of 59.4, 45.3, 47.8 kcal/mol, respectively, to form a complex. This means the repulsive force between anion Cu^- and $[C_6H_5Cu_mH]^-$ ($m = 1-3$) are very strong. And what's more, the $[CuH]^-$ would has been involved in the products if this pathway happened, while it is not detected by the experiment. Therefore, this pathway is very difficult to take place and could be ruled out safely.

On the basis of analysis above, the intermediate $[C_6H_5Cu_mH]^-$ ($m = 1-3$) releasing H to neutral Cu is turned out to be the most energetically favorable. In addition, it is worth mentioning that the yielded complexes $[C_6H_5Cu_m]^-$ ($m = 1-3$) may go on interacting with another neutral Cu to form the complex $[C_6H_5Cu_m]^-$ ($m = 2-4$). Moreover, these reactions are thermodynamically controlled for $\Delta E < 0$ and $\Delta G < 0$.

5. Conclusions

The phenyl−copper metal (atoms or clusters) complexes are produced from laser vaporization. A combined experimental and theoretical effort is made to elucidate the binding patterns, structures, and formation mechanism of these species. EAs of $[Cu_mC_6H_5]^-$ ($m = 2, 3$) are obtained from the photoelectron spectrum at 308 nm photon and theoretical calculation. Experimental and theoretical results are excellent co-incident with each other. The optimized ground-state structures of complex $[C_6H_5Cu]^-$ and $[C_6H_5Cu_2]^-$ possess C_{2v} ground-state structures and the obtained complex $[C_6H_5Cu_3]^-$ has two C_{2v} isomeric structures. Moreover, the comparisons between the observed spectrum of these complexes and the pure copper clusters suggest that the C_6H_5 group acts just like an additional copper atom in the clusters and contributes a single electron to bond with the copper fragment through C−Cu σbond. Considering the recent studies on the properties of $[C_6H_5M_m]^-$(M═Ag, Au, $m = 1-3$), it could be concluded that all these three coinage metal complexes $[C_6H_5M_m]^-$($m = 1-3$) possess C_{2v} symmetry structure.

The formation mechanisms of $[Cu_mC_6H_5]^-$($m = 1-3$) from the reaction between benzene and $[Cu_m]^-$($m = 1-3$) have been studied at the B3LYP//6-311G(d, p)/Lanl2dz levels. The calculation results indicate that all the three reactions proceed through two consecutive steps. The first step is the formation of intermediate complex $[C_6H_5Cu_mH]^-$ ($m = 1-3$) via an insertion reaction with the cleavage of C−H bond and the formation of Cu−H bond simultaneously. The second step yields the product of $[C_6H_5Cu_m]^-$ ($m = 1-3$) with the releasing of H. The pathway of H releasing to neutral Cu has been turned out to be the most favorable energetically. Moreover, as compared with energy barrier of TS (a rate-limiting step) in first step and the energy difference ΔE of H removed by neutral Cu in second step, respectively, it has been found that the product $[C_6H_5Cu_2]^-$ is easier to be yielded than the species of $[C_6H_5Cu_3]^-$ and $[C_6H_5Cu]^-$ in turn. It is in well agreement with the experiment findings that $[C_6H_5Cu_2]^-$ is the predominant complex observed by the mass spectra and in turn is $[C_6H_5Cu_3]^-$ and $[C_6H_5Cu]^-$.

Acknowledgment. This work was supported by NSFC (20373071, 20573110). Most calculations have been done at Virtual Laboratory for Computational Chemistry, CNIC, CAS.

References and Notes

(1) Xu, Z.; Xiao, F. S.; Purnell, S. K.; Alexeev, O.; Kawi, S.; Deutsch, S. E.; Gates, B. C. *Nature (London)* **1994**, *372*, 346.
(2) Whitten, J. L.; Yang, H. *Surf. Sci. Rep.* **1996**, *24*, 55.
(3) Toshima, N.; Yonezawa, T. *New J. Chem.* **1998**, *22*, 1179.
(4) Nakanishi, W.; Yamanaka, M.; Nakamura, E. *J. Am. Chem. Soc.* **2005**, *127*, 1446.
(5) Fanta, P. E. *Chem. Rev.* **1964**, *64*, 613.
(6) Hoshino, K.; Kurikawa, T.; Takeda, H.; Nakajima, A.; Kaya, K. *J. Phys. Chem.* **1995**, *99*, 3053.
(7) Kurikawa, T.; Hirano, M.; Takeda, H.; Yagi, K.; Hoshino, K.; Nakajima, A.; Kaya, K. *J. Phys. Chem.* **1995**, *99*, 16248.
(8) Kurikawa, T.; Takeda, H.; Hirano, M.; Judai, K.; Arita, T.; Nagao, S.; Nakajima, A.; Kaya, K. *Organometallics* **1999**, *18*, 1430.
(9) Gerhards, M.; Thomas, O. C.; Nilles, J. M.; Zheng, W. J.; Bowen, K. H., Jr. *J. Chem. Phys.* **2002**, *116*, 10247.
(10) Xing, X. P.; Tian, Z. X.; Liu, H. T.; Tang, Z. C. *J. Phys. Chem. A* **2003**, *107*, 8484.
(11) Zheng, W. J.; Nilles, J. M.; Thomas, O. C.; Bowen, K. H., Jr. *J. Chem. Phys.* **2005**, *122*, 44306.
(12) Zheng, W. J.; Nilles, J. M.; Thomas, O. C.; Bowen, K. H., Jr. *Chem. Phys. Lett.* **2005**, *401*, 266.
(13) Pandey, R.; Rao, B. K.; Jena, P.; Blanco, M. A. *J. Am. Chem. Soc.* **2001**, *123*, 3799.
(14) Rao, B. K.; Jena, P. *J. Chem. Phys.* **2002**, *117*, 5234.
(15) Kandalam, A. K.; Rao, B. K.; Jena, P.; Pandey, R. *J. Chem. Phys.* **2004**, *120*, 10414.
(16) Wu, D. Y.; Ren, B.; Jiang, Y. X.; Xu, X.; Tian, Z. Q. *J. Phys. Chem. A* **2002**, *106*, 9042.
(17) Socaciu, L. D.; Hagen, J.; Bernhardt, T. M.; Wöste, L.; Heiz, U.; Häkkinen, H.; Landman, U. *J. Am. Chem. Soc.* **2003**, *125*, 10437.
(18) Wallace, W. T.; Whetten, R. L. *J. Am. Chem. Soc.* **2002**, *124*, 7499.
(19) Stolcic, D.; Fischer, M.; Ganteför, G.; Kim, Y. D.; Sun, Q.; Jena, P. *J. Am. Chem. Soc.* **2003**, *125*, 2848.
(20) Sun, S. T.; Xing, X. P.; Liu, H. T.; Tang, Z. C. *J. Phys. Chem. A* **2005**, *109*, 11742.
(21) Xing, X. P.; Liu, H. T.; Tang, Z. C. *Phys. Chem. Comm.* **2003**, *6*, 32.
(22) Xing, X. P.; Tian, Z. X.; Liu, P.; Gao, Z.; Zhu, Q. H.; Tang, Z. C. *Chin. J. Chem. Phys.* **2002**, *15*, 83.
(23) Frisch, M. J.; Trucks, G. W.; Schlegel, H. B.; Scuseria, G. E.; Robb, M. A.; Cheeseman, J. R.; Montgomery, J. A., Jr.; Vreven, T.; Kudin, K. N.; Burant, J. C.; Millam, J. M.; Iyengar, S. S.; Tomasi, J.; Barone, V.;Mennucci, B.; Cossi, M.; Scalmani, G.; Rega, N.; Petersson, G. A.; Nakatsuji, H.; Hada, M.; Ehara, M.; Toyota, K.; Fukuda, R.; Hasegawa, J.; Ishida, M.; Nakajima, T.; Honda, Y.; Kitao, O.; Nakai, H.; Klene, M.; Li, X.; Knox, J. E.; Hratchian, H. P.; Cross, J. B.; Bakken, V.; Adamo, .; Jaramillo, J.; Gomperts, R.; Stratmann, R. E.; Yazyev, O.; Austin, A. J.; Cammi, R.; Pomelli, C.; Ochterski, J. W.; Ayala, P. Y.; Morokuma, K.;Voth, G. A.; Salvador, P.; Dannenberg, J. J.; Zakrzewski, V. G.; Dapprich, S.; Daniels, A. D.; Strain, M. C.; Farkas, O.; Alick, D. K.; Rabuck, A. D.; Raghavachari, K.; Foresman, J. B.; Ortiz, J. V.; Cui, Q.; Baboul, A. G.; Clifford, S.; Cioslowski, J.; Stefanov, B. B.; Liu, G.; Liashenko, A.; Piskorz, P.; Komaromi, I.; Martin, R. L.; Fox, D. J.; Keith, T.; Al-Laham, M. A.; Peng, C. Y.; Nanayakkara, A.; Challacombe, M.; Gill, P. M. W.; Johnson, B.; Chen, W.; Wong, M. W.; Gonzalez, C.; Pople, J. A. *Gaussian 03*, revision C.02 ed.; Gaussian, Inc.: Wallingford, CT, 2004.
(24) (a) Lee, C.; Yang, W.; Parr, R. G. *Phys. Rev.* **1988**, *B37*, 785. (b) Becke, A. D. *J. Chem. Phys.* **1993**, *98*, 1372, 5648. (c) Becke, A. D. *Phys. Rev.* **1988**, *A38*, 3098.
(25) Wadt, W. R.; Hay, P. J. *J. Chem. Phys*. **1985**, *82*, 284.
(26) Legge, F. S.; Nyberg, G. L.; Peel, J. B. *J. Phys. Chem. A* **2001**, *105*, 7905.
(27) Sanchez, A.; Abbet, S.; Heiz, U.; Schneider, W. D.; Häkkinen, H.; Barnett, R. N.; Landman, U. *J. Phys. Chem. A* **1999**, *103*, 9573.
(28) Yamanaka, M.; Inagaki, A.; Nakamura, E. *J. Comput. Chem*. **2003**, *24*, 1401.
(29) (a) Cioslowski, J. *J. Am. Chem. Soc.* **1989**, *111*, 8333. (b) Cioslowski, J. *Phys. Re*V. *Lett.* **1989**, *62*, 1469.
(30) De Oliveira, A. E.; Haiduke, R. L. A.; Burns, R. E. *J. Phys. Chem. A* **2000**, *104*, 5320.
(31) Ho, J.; Ervin, K. M.; Lineberger, W. C. *J. Chem. Phys.* **1990**, *93*, 6987.
(32) Taylor, K. J.; Pettiette-Hall, C. L.; Cheshnovsky, O.; Smalley, R. E. *J. Chem. Phys.* **1992**, *96*, 3319.
(33) Bauschlicher, C. W., Jr.; Langhoff, S. R.; Taylor, P. R. *J. Chem. Phys.* **1988**, *88*, 1041.
(34) Bauschlicher, C. W., Jr.; Langhoff, S. R.; Partridge, H. *J. Chem. Phys.* **1989**, *91*, 2412.
(35) Leopold, D. G.; Ho, J.; Lineberger, W. C. *J. Chem. Phys.* **1987**, *86*, 1715.
(36) Ho, J.; Ervin. K. M.; Lineberger, W. C. *J. Chem. Phys.* **1990**, *93*, 6987.
(37) Li, J.; Li, X.; Zhai, H. J.; Wang, L. S. *Science* **2003**, *299*, 864.
(38) Wang, B. L.; Zhao, J. J.; Chen, X. S.; Shi, D. N.; Wang, G. H. *Phys. Rev. A* **2005**, *71*, 033201.

(39) Häkkinen, H.; Moseler, M.; Kostko, O.; Morgner, N.; Hoffmann, M. A.; Issendorff, B. V. *Phys. Rev. Lett.* **2004**, *93*, 93401.
(40) Häkkinen, H.; Yoon, B.; Landman, U.; Li, X.; Zhai, H. J.; Wang, L. S. *J. Phys. Chem. A* **2003**, *107*, 6168.
(41) Häkkinen, H.; Moseler, M.; Landman, U. *Phys. Rev. Lett.* **2002**, *89*, 33401.
(42) Li, X.; Kiran, B.; Li, J.; Zhai, H. J.; Wang, L. S. *Angew. Chem., Int. Ed* **2002**, *41*, 4786.
(43) Liu, H. T.; Xing, X. P.; Sun, S. T.; Gao, Z.; Tang, Z. C. *J. Phys. Chem. A* **2006**, *110*, 8688.
(44) Tozer, D. J.; Handy, N. C. *J. Chem. Phys.* ***1998***, 109, 10180.
(45) Antes, I.; Frenking, G. *Organometallics* **1995**, *14*, 4263.